

**$^{87}\text{Rb}$  NMR study of the paraelectric-antiferroelectric phase transition in  $\text{Rb}_{0.52}(\text{ND}_4)_{0.48}\text{D}_2\text{AsO}_4$** 

R. Blinc, J. Dolinšek, and B. Zalar

*Jožef Stefan Institute, E. Kardelj University of Ljubljana, Ljubljana, Yugoslavia*

A. Fuith and H. Warhanek

*Institut für Experimentalphysik, Universität Wien, A-1090 Wien, Austria*

(Received 9 June 1989; revised manuscript received 1 October 1989)

$^{87}\text{Rb}$   $\frac{1}{2} \rightarrow -\frac{1}{2}$  NMR line shape and spin-lattice relaxation time ( $T_1$ ) data demonstrate the presence of a first-order transition from a paraelectric (PE) to an antiferroelectric (AFE) phase in substitutionally disordered  $\text{Rb}_{0.52}(\text{ND}_4)_{0.48}\text{D}_2\text{AsO}_4$  where the PE and AFE lines overlap between 140 and 135 K. The  $^{87}\text{Rb}$  site symmetry is compatible with the  $I\bar{4}2d$  symmetry above  $T_c$  and with the  $P2_12_1$  symmetry of pure  $\text{ND}_4\text{D}_2\text{AsO}_4$  below  $T_c$ . Superimposed on the glassy order that produces an inhomogeneous broadening of the  $^{87}\text{Rb}$  NMR lines is a dynamic disorder of the deuterons in the  $\text{O}-\text{D}\cdots\text{O}$  bonds above  $T_c$  and an antiferroelectric long-range order below  $T_c$ . The  $\text{O}-\text{D}\cdots\text{O}$  dynamics is driven by an antiferroelectric soft mode which freezes out at  $T_c$  and determines the  $^{87}\text{Rb}$   $T_1$ .

**I. INTRODUCTION**

It has been recently shown<sup>1,2</sup> that substitutionally disordered mixed crystals  $\text{Rb}_{1-x}(\text{ND}_4)_x\text{D}_2\text{AsO}_4$ —henceforth designated as RADA—of ferroelectric (FE)  $\text{RbD}_2\text{AsO}_4$  and antiferroelectric (AFE)  $\text{ND}_4\text{D}_2\text{AsO}_4$  represent a frustrated H-bonded system with randomly competing interactions.<sup>3</sup> For pure  $\text{RbD}_2\text{AsO}_4$  the ferroelectric transition takes place at  $T_c=178$  K whereas the antiferroelectric transition in pure  $\text{ND}_4\text{D}_2\text{AsO}_4$  occurs at  $T_c=304$  K. The system shows for small  $x$  a paraelectric-ferroelectric (PE-FE) and for large  $x$  a paraelectric-antiferroelectric (PE-AFE) transition. For intermediate  $x$  values no long-range ordering takes place and the system forms at low temperatures a “proton” or “deuteron” dipolar glass.<sup>4,5</sup> In contrast to isomorphous  $\text{Rb}_{1-x}(\text{ND}_4)_x\text{D}_2\text{PO}_4$  (Refs. 4 and 5) the phase diagram is not symmetric<sup>2</sup> as the paraelectric-antiferroelectric transition temperature is much higher than the paraelectric-ferroelectric one.

In order to throw some light on the nature of these transitions and the local ordering at the antiferroelectric side of the phase diagram<sup>1,2</sup> we decided to perform a  $^{87}\text{Rb}$  NMR study of  $\text{Rb}_{0.52}(\text{ND}_4)_{0.48}\text{D}_2\text{AsO}_4$ . We particularly hoped to determine the interplay between the incipient glassy order and the long-range antiferroelectric order. We wanted to see as well if the  $\text{O}-\text{D}\cdots\text{O}$  dynamics is of the glassy type and exhibits a Bloembergen-Purcell-Pound (BPP) like  $T_1$  minimum<sup>6</sup> or is determined by an antiferroelectric soft mode as in pure  $\text{ND}_4\text{D}_2\text{AsO}_4$ .

The experiments were performed on a deuterated RADA crystal with an ammonium concentration of  $x=0.48$  as determined by flame spectroscopy and a degree of deuteration of about 90% as determined by mass spectroscopy. The  $^{87}\text{Rb}$   $\frac{1}{2} \rightarrow -\frac{1}{2}$  spectra were measured at 88.34 MHz. A Fourier transform  $(90^\circ)_x - (90^\circ)_y$  solid-echo technique was used. The homogeneous linewidth

was determined from the slope of the spin-echo amplitude versus pulse separation plot.

**II. THEORY**

The phase diagram of the  $\text{Rb}_{1-x}(\text{ND}_4)_x\text{D}_2\text{AsO}_4$  system can be described by the random bond Ising model<sup>3</sup>

$$\mathcal{H} = -\frac{1}{2} \sum_{i,j} J_{ij} S_i^z S_j^z, \quad (1)$$

where the pseudospin variable  $S^z = \pm 1$  describes the two possible deuteron sites in the  $\text{O}-\text{D}\cdots\text{O}$  bonds and the random interactions  $J_{ij}$  are distributed according to a Gaussian probability density

$$P(J_{ij}) = \left[ \frac{1}{2\pi J^2} \right]^{-1/2} \exp[-(J_{ij} - J_0)^2 / (2J^2)]. \quad (2)$$

The  $J_{ij}$  are assumed<sup>3</sup> to be infinitely ranged with a mean  $J_0 = \bar{J}_0/N$  and a variance  $J = \bar{J}/N^{1/2}$ . Here  $N$  is the number of pseudospin sites.  $\bar{J}_0$  and  $\bar{J}$  are both concentration dependent,

$$\bar{J}_0(x) = -\bar{J}_0^{\text{AFE}}x + \bar{J}_0^{\text{FE}}(1-x) \quad (3)$$

and

$$\bar{J}(x) = 2[x(1-x)]^{1/2}\bar{J}_{0.5}. \quad (4)$$

Here  $\bar{J}_0^{\text{AFE}} > 0$  and  $\bar{J}_0^{\text{FE}} > 0$  are parameters appropriate for pure  $\text{ND}_4\text{D}_2\text{AsO}_4$  and  $\text{RbD}_2\text{AsO}_4$ , whereas  $\bar{J}_{0.5}$  characterizes the 50% DRbDA-DADA mixture.

For  $|\bar{J}_0| > \bar{J}$  a transition from a paraelectric into a ferroelectric ( $\bar{J}_0 > 0$ ) or antiferroelectric ( $\bar{J}_0 < 0$ ) phase appears, whereas for  $\bar{J} \geq |\bar{J}_0|$  the transition is from a paraelectric into a pseudospin glass phase with zero long-range order  $p = 1/N \sum_i \langle S_i^z \rangle$ , but non-zero Edwards-Anderson glassy order parameter  $q = 1/N \sum_i \langle S_i^z \rangle^2$ .

If  $|\tilde{J}_0| > \tilde{J}$  and  $\tilde{J}_0 < 0$  as expected for  $\text{Rb}_{0.52}(\text{ND}_4)_{0.48}\text{D}_2\text{AsO}_4$ , we should have a paraelectric-antiferroelectric transition with nonzero long-range order (i.e., "staggered polarization"  $p \neq 0$ ) below  $T_c$ . This should exist in addition to the pseudospin-glass order represented by  $q$ .

In analogy to  $\text{Rb}_{1-x}(\text{ND}_4)_x\text{D}_2\text{PO}_4$  we now add to expression (1) a random field term  $-\sum_i S_i^z f_i$ . The random fields  $f_i$  are as well distributed according to a Gaussian probability density with a variance  $\Delta$  and zero mean value.

The two order parameters  $p$  and  $q$  are determined by the coupled self-consistent equations

$$p = \int_{-\infty}^{+\infty} \frac{dz}{\sqrt{2\pi}} e^{-z^2/2} \tanh[\beta(\tilde{J}\sqrt{Q}z + |\tilde{J}_0|p)], \quad (5a)$$

$$q = \int_{-\infty}^{+\infty} \frac{dz}{\sqrt{2\pi}} e^{-z^2/2} \tanh^2[\beta(\tilde{J}\sqrt{Q}z + |\tilde{J}_0|p)]. \quad (5b)$$

Here  $\beta = 1/(kT)$  and  $Q = q + \Delta/\tilde{J}^2$ . The temperature dependences of  $p$  and  $q$  expected on the basis of Eqs. (5a) and (5b) are schematically shown in Fig. 1. We see that  $q$  is—for  $\Delta \neq 0$ —different from zero at all temperatures whereas  $p$  is nonzero only below  $T_c$ . It should be noted that the temperature dependence of  $q$  is below  $T_c$  strongly affected by the temperature dependence of  $p$ .

The relation between the NMR frequency  $\nu_i$  at a given Rb site and the local O—D  $\cdots$  O bond polarization  $p_i = \langle S_i^z \rangle$  can be written as

$$\nu_i = \nu_0 + \sum_j C_{ij} \langle S_j^z \rangle. \quad (6)$$

The presence of glassy order will result in an inhomogeneous broadening of the Rb line. The second moment of the inhomogeneously broadened line is above  $T_c$  proportional to the Edwards-Anderson glassy order parameter  $q$

$$M_2 = \int f(\nu)(\nu - \nu_0)^2 d\nu \\ = \frac{1}{N_{\text{Rb}}} \sum_i \sum_{jk} [C_{ij} C_{ik} \langle S_j^z \rangle \langle S_k^z \rangle]_{\text{av}} = Cq, \quad T > T_c \quad (7)$$

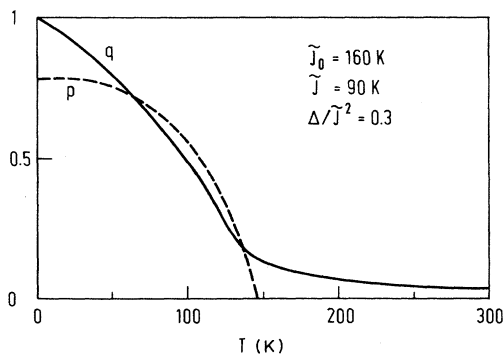


FIG. 1. Temperature dependences of the glassy order parameter  $q$  and the long-range order parameter  $p$  according to Eqs. (5a) and (5b) for  $\tilde{J}_0 = 160$  K,  $\tilde{J} = 90$  K, and  $\Delta/\tilde{J}^2 = 0.3$ .

where  $C = 1/N_{\text{Rb}} \sum_i \sum_j C_{ij}^2$ . Here  $[\cdots]_{\text{av}}$  denotes the disorder average, i.e., the simultaneous average over random bonds and random fields.

The center of gravity  $\bar{\nu} = \int f(\nu)\nu d\nu$  of the NMR lines is in this case proportional to the long-range order parameter  $p$ ,

$$\bar{\nu} = \nu_0, \quad T > T_c \quad (p = 0) \quad (8a)$$

$$\bar{\nu} = \nu_0 + \nu_1 p, \quad T < T_c \quad (p \neq 0). \quad (8b)$$

If higher-order terms are added to the expansion (6), one sees that above  $T_c$  the center of gravity of the NMR line  $\bar{\nu}$  is proportional to  $q$  and is thus not really  $T$ -independent as predicted by Eq. (8a).

### III. RESULTS AND DISCUSSION

The effect of substitutional disorder and the incipient glass ordering lead to a large inhomogeneous broadening of the  $^{87}\text{Rb } \frac{1}{2} \rightarrow -\frac{1}{2}$  NMR line even at room temperature. The inhomogeneous broadening is strongly anisotropic, increases with decreasing temperature, and becomes as high as 20 kHz at some orientations (Fig. 2). The homogeneous linewidth on the other hand is only  $\approx 300$  Hz. In agreement with the average site symmetry of the paraelectric phase  $\bar{4}2m$  there is just a single  $^{87}\text{Rb } \frac{1}{2} \rightarrow -\frac{1}{2}$  NMR line at room temperature in the rotation spectrum. The average  $^{87}\text{Rb}$  electric field gradient (EFG) tensor is axially symmetric ( $\eta = 0$ ) and the principle axes ( $X, Y, Z$ ) are parallel to the crystal axes  $x, y, z$ . The largest principle axis  $Z$  is parallel to the crystal  $z$  axis.

On lowering the temperature, the NMR line continuously broadens down to 140 K where a new broad line starts to grow out of the noise (Fig. 3). The new line coexists with the paraelectric line down to 132 K where the paraelectric line disappears. The new line thus belongs to the low-temperature phase. This behavior is quite analogous to the one observed in  $\text{Rb}_{0.22}(\text{ND}_4)_{0.78}\text{D}_2\text{PO}_4$  (Ref. 8) where a paraelectric-antiferroelectric phase transition takes place as well.

The relative intensities of the two lines—i.e., the volume fractions of the paraelectric and antiferroelectric phases—are plotted versus temperature in Fig. 4. The coexistence of the two phases over a range of nearly 8 K demonstrates that we deal in  $\text{Rb}_{0.52}(\text{ND}_4)_{0.48}\text{D}_2\text{AsO}_4$  with a first-order phase transition from the PE to the AFE phase.

The normalized frequency shift  $(\bar{\nu} - \nu_0)/\nu_1$  of the  $^{87}\text{Rb } \frac{1}{2} \rightarrow -\frac{1}{2}$  transition is plotted versus temperature in Fig. 5. Here  $\nu_1$  is the limiting value of the shift  $\bar{\nu} - \nu_0$  for  $T \rightarrow 0$ . Above  $T_c \approx 140$  K  $(\bar{\nu} - \nu_0)/\nu_1$  varies only slightly with temperature. At  $T_c$   $(\bar{\nu} - \nu_0)/\nu_1$  jumps from about 0.02 to about 0.85 demonstrating the sudden onset of the long-range order characteristic for a phase transition of first order. Below  $T_c$   $(\bar{\nu} - \nu_0)/\nu_1$  continues to increase with decreasing temperature as expected for a situation where the long-range order parameter  $p$  (i.e., the "staggered" polarization) is not yet saturated.

It should be noted that if the relation between  $\nu_i$  and  $p_i = \langle S_i^z \rangle$  would be strictly linear—as given by Eq. (6)—

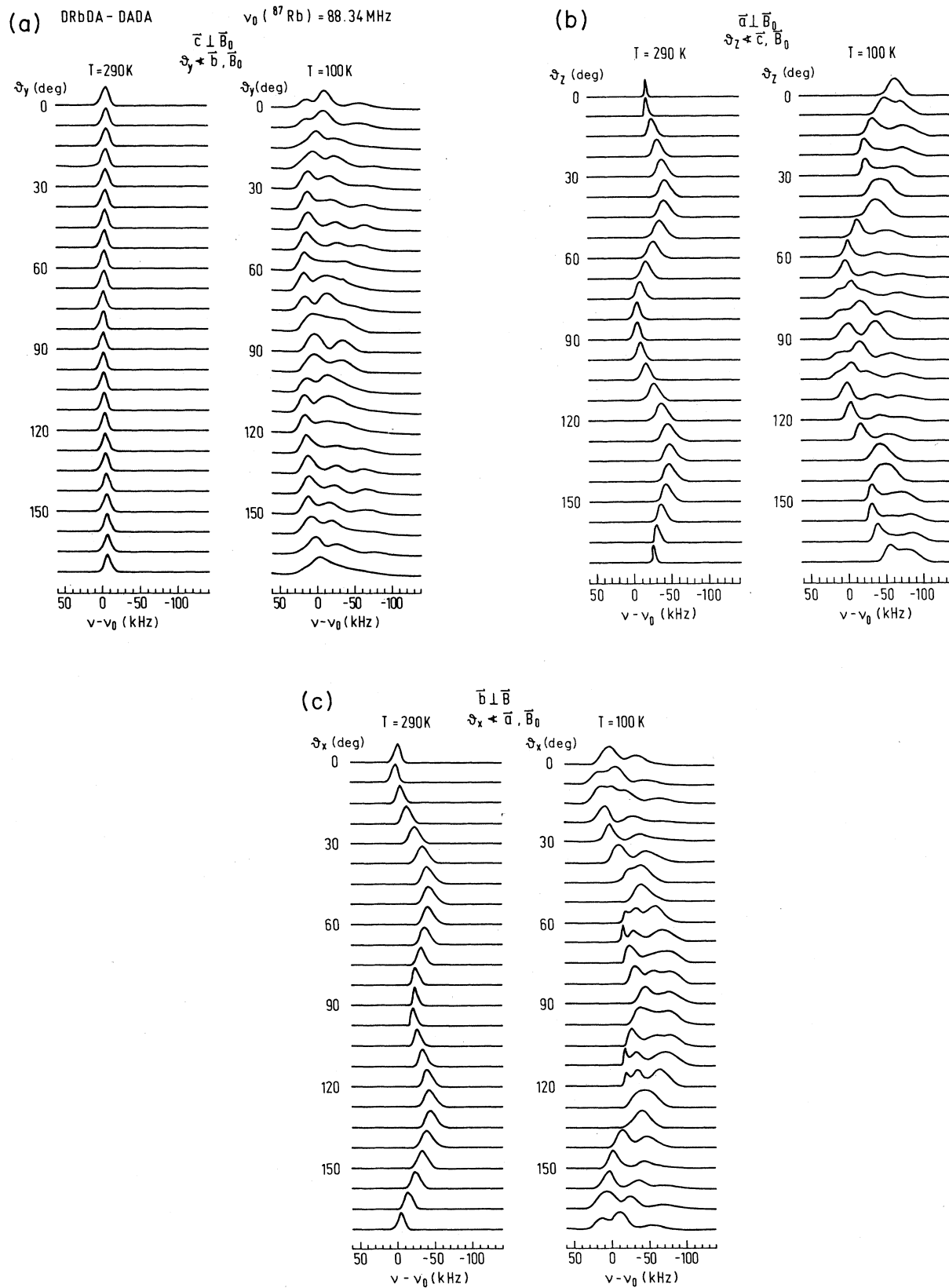


FIG. 2. Angular dependence of the  $^{87}\text{Rb} \frac{1}{2} \rightarrow -\frac{1}{2}$  NMR line shapes at 290 and 100 K.

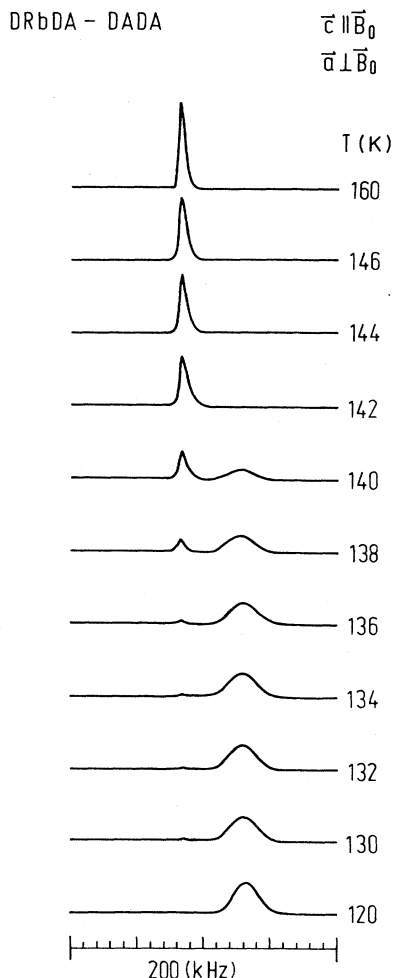


FIG. 3. Temperature dependence of the  $^{87}\text{Rb } \frac{1}{2} \rightarrow -\frac{1}{2}$  NMR spectra at  $c \parallel \mathbf{B}_0$ ,  $\mathbf{a} \perp \mathbf{B}_0$  in the region of the paraelectric-antiferroelectric phase transition.

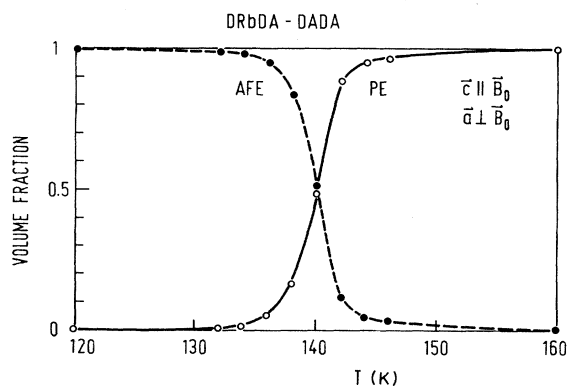


FIG. 4. Temperature dependence of the volume fractions of the paraelectric (solid line) and antiferroelectric (dashed line) phases in the region of the paraelectric-antiferroelectric phase transition.

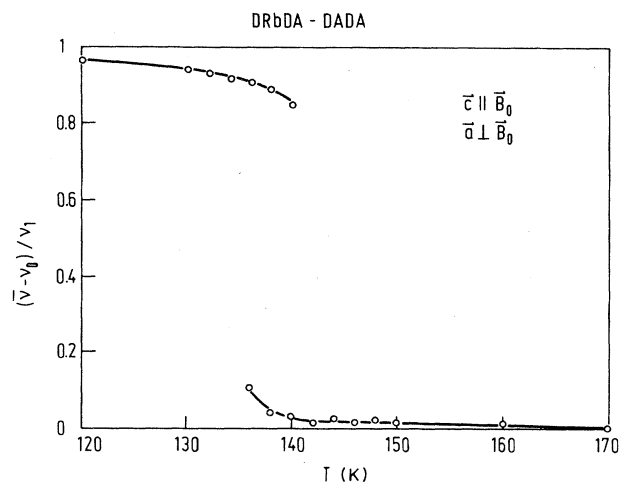


FIG. 5. Normalized frequency shift  $(\bar{\nu} - \nu_0) / \nu_1$  of the  $^{87}\text{Rb } \frac{1}{2} \rightarrow -\frac{1}{2}$  transition vs temperature for  $c \parallel \mathbf{B}_0$ ,  $\mathbf{a} \perp \mathbf{B}_0$ .

the temperature dependence of  $(\bar{\nu} - \nu_0) / \nu_1$  would be identical to the temperature dependence of  $p$ .

The temperature dependences of the second moment  $M_2$  of the  $^{87}\text{Rb } \frac{1}{2} \rightarrow -\frac{1}{2}$  NMR line is presented in Fig. 6. Whereas above  $T_c$   $(\bar{\nu} - \nu_0) / \nu_1$  is only weakly temperature dependent,  $M_2$  strongly increases with decreasing temperature over most of the paraelectric phase, similarly as the Edwards-Anderson order parameter  $q$  in the presence of random fields. At  $T_c$  there is a discontinuous increase in  $M_2$  which reflects the increase in  $q$  due to the discontinuous increase in  $p$  as well as the splitting in the  $^{87}\text{Rb}$  spectrum.

In view of the first-order nature of the PE-AFE phase transition the experimental  $T$  dependence of  $(\bar{\nu} - \nu_0) / \nu_1$  and  $M_2$  cannot be quantitatively compared with the theoretical  $T$  dependences of  $p$  and  $q$  (Fig. 1) as described

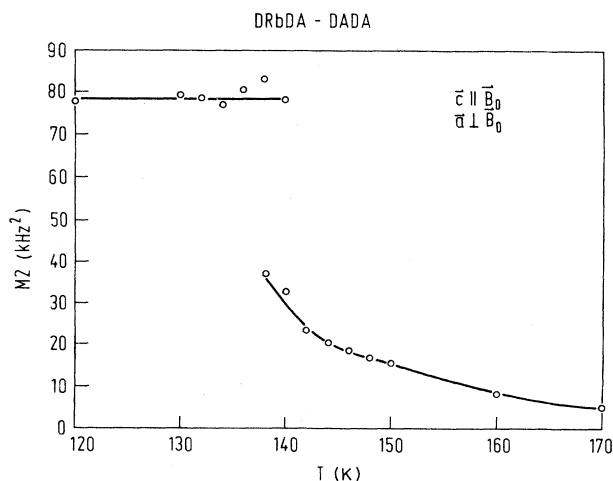


FIG. 6. Second moment of the  $^{87}\text{Rb } \frac{1}{2} \rightarrow -\frac{1}{2}$  NMR line vs temperature.

by Eqs. (5a) and (5b). These equations are appropriate for the case of a transition of second order and not for a transition of first order. The first-order nature of the transition in  $\text{Rb}_{1-x}(\text{ND}_4)_x\text{D}_2\text{AsO}_4$  is the result of four spin interaction terms<sup>7</sup> which are not contained in the random bond-random field Ising model Hamiltonian<sup>3</sup> leading to expressions (5a) and (5b).

In the low-temperature phase below  $T_c$  up to four  $^{87}\text{Rb}$  lines can be resolved at some orientations. The maxima of these lines give rise to a rotation pattern from which four different  $^{87}\text{Rb}$  EFG tensors can be calculated. The EFG tensors have the same eigenvalues but different orientations with respect to the crystal axes. In all four tensors the largest principal axis  $Z$  is no longer parallel to the crystal  $z\parallel c$  axis. The average tilt angle of the principal  $Z$  axis with respect to the  $c$  axis of the crystal is about  $20^\circ$ . The distribution of the tilt angles around the mean value—which can be approximated by a Gaussian with a root-mean-square deviation of  $\approx 5^\circ$ —is, as in  $\text{Rb}_{1-x}(\text{ND}_4)_x\text{D}_2\text{PO}_4$ ,<sup>8</sup> the main source of the glassy type inhomogeneous broadening of the  $^{87}\text{Rb}$  lines. The general orientation of the four EFG tensors with respect to the crystal axes and the fact that the asymmetry parameter  $\eta = (V_{XX} - V_{YY})/V_{ZZ}$  is now different from zero ( $\eta \approx 0.2$ ) shows that the site symmetry  $\bar{4}$  and the two glide mirror planes  $d_a$  and  $d_b$  of the paraelectric phase are lost at the Rb sites. This is compatible with the  $P2_12_12_1$  space group of the antiferroelectric phase of pure  $\text{ND}_4\text{D}_2\text{AsO}_4$ .<sup>7</sup>

It should be mentioned that whereas the four low-temperature EFG tensors clearly reflect the local symmetry of the antiferroelectric phase the relation between them is still given by the symmetry operation  $\bar{4}2m$ , i.e., by the full symmetry of the paraelectric phase. This higher apparent symmetry of the rotation pattern thus reflects the existence of  $90^\circ$  domains which are related by the symmetry elements lost at  $T_c$ .

The temperature dependence of the  $^{87}\text{Rb}$   $\frac{1}{2} \rightarrow -\frac{1}{2}$  spin-lattice relaxation time  $T_1$  is shown in Fig. 7 for  $c\parallel B_0, a\perp B_0$ . On cooling down from room temperature  $T_1$  first increases, reaches a maximum of about 30 ms at 260 K and then decreases down to about 2 ms in the 140–130 K range. At  $T_c$ ,  $T_1$  discontinuously increases by a factor of  $\approx 15$  and then continues to increase gradually with decreasing temperature.

It should be stressed that in the range where the paraelectric and ferroelectric lines coexist the  $T_1$  of the paraelectric line is short and the  $T_1$  of the antiferroelectric line is long. The shape of the  $T_1$  versus  $10^3/T$  plot is again similar to the one observed in  $\text{Rb}_{0.22}(\text{ND}_4)_{0.78}\text{D}_2\text{PO}_4$ ,<sup>8</sup> but very different from the one observed in the deuteron glass  $\text{Rb}_{0.5}(\text{ND}_4)_{0.5}\text{D}_2\text{PO}_4$ .<sup>6</sup> The absence of a broad asymmetric minimum in the  $T_1$  versus  $10^3/T$  plot, in particular, proves that we do not deal here with a glassy freeze out of the motion of the

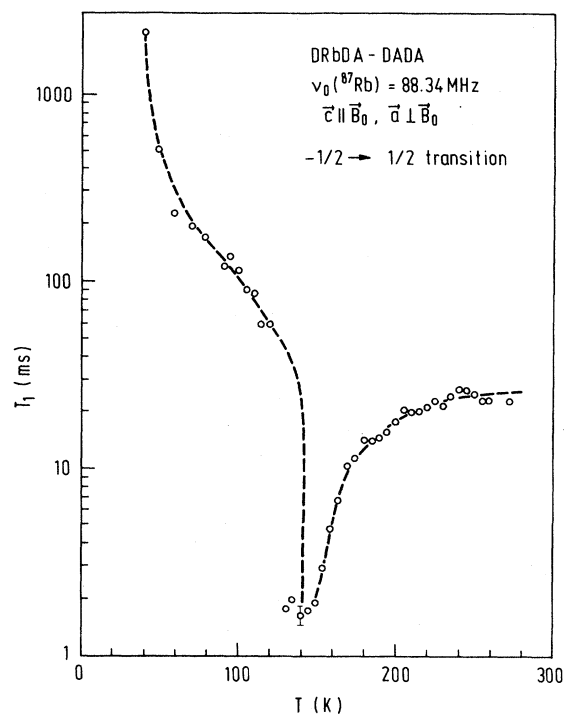


FIG. 7. Temperature dependence of the  $^{87}\text{Rb}$   $\frac{1}{2} \rightarrow -\frac{1}{2}$  spin-lattice relaxation time  $T_1$  in the region  $T_c$ .

deuterons between the two potential minima in the  $\text{O}-\text{D}\cdots\text{O}$  bond but rather with a condensing antiferroelectric soft mode as in  $\text{ND}_4\text{D}_2\text{PO}_4$ .<sup>7</sup>

The temperature dependence of the  $^{87}\text{Rb}$   $T_1$  around  $T_c$  can be explained by the same condensing soft-mode model as in other  $\text{KD}_2\text{PO}_4$  and  $\text{ND}_4\text{D}_2\text{PO}_4$  crystals.<sup>7</sup> We thus see that superimposed on the glassy order,<sup>3</sup> which produces the inhomogeneous broadening of the NMR lines, there is a dynamic disorder of the deuterons in the  $\text{O}-\text{D}\cdots\text{O}$  bonds. The dynamic disorder is driven by the antiferroelectric soft mode which determines the Rb  $T_1$  and freezes out at  $T_c$ . The freeze out of the soft mode results in long-range antiferroelectric ordering of the  $\text{O}-\text{D}\cdots\text{O}$  deuterons and the formation of  $90^\circ$  domains as predicted by the Slater-Takagi model<sup>7</sup> of  $\text{KH}_2\text{PO}_4$  and  $\text{NH}_4\text{H}_2\text{PO}_4$  type crystals.

#### ACKNOWLEDGMENTS

This work was supported by the Österreich. Fonds zur Förderung der wissenschaftlichen Forschung under Project No. P 6758 P. One of the authors (R.B.) would like to thank the University of Vienna for the hospitality and support extended to him during his visit to this institution when this work was started.

- <sup>1</sup>Z. Trybula, J. Stankowski, and R. Blinc, *Ferroelectric Lett.* **6**, 57 (1986).
- <sup>2</sup>Z. Trybula, J. Stankowski, L. Szczepanska, R. Blinc, A. Weiss, and N. S. Dalal, *Physica B* **153**, 143 (1988).
- <sup>3</sup>B. Tadić, R. Pirc, and R. Blinc, *Phys. Rev. B* **37**, 679 (1988).
- <sup>4</sup>E. Courtens, *Jpn. J. Appl. Phys.* **24**, Suppl. 24-2, 70 (1985), and references therein.
- <sup>5</sup>A. Terauchi, *Jpn. J. Appl. Phys.* **24**, Suppl. 24-2, 75 (1989).
- <sup>6</sup>R. Blinc, D. C. Ailion, B. Günther, and S. Žumer, *Phys. Rev. Lett.* **57**, 2826 (1986).
- <sup>7</sup>See, for instance, R. Blinc and B. Žekš, *Soft Modes in Ferroelectrics and Antiferroelectrics* (North-Holland, Amsterdam, 1974), and references therein.
- <sup>8</sup>R. Kind, O. Liechti, R. Brüsweiler, J. Dolinšek, and R. Blinc, *Phys. Rev. B* **36**, 13 (1987).